

# Superplasticity of Yttria-Stabilized Tetragonal ZrO<sub>2</sub> Polycrystals

FUMIHIRO WAKAI,\* SHUJI SAKAGUCHI, and YOSOO MATSUNO  
Government Industrial Research Institute, Nagoya 462, Japan

*The uniaxial tensile deformation behavior of 3 mol% Y<sub>2</sub>O<sub>3</sub>-tetragonal ZrO<sub>2</sub> polycrystals (Y-TZP, grains  $\leq 0.3 \mu\text{m}$ ) was studied at temperatures up to 1500°C in ambient atmosphere. The tensile specimens which were elongated at constant displacement rates from  $1.1 \times 10^{-4} \text{ s}^{-1}$  to  $5.5 \times 10^{-4} \text{ s}^{-1}$  at 1450°C exhibited the unusually large deformation (over 120% by nominal strain). The superplastically deformed specimens retained a bending strength of 976 MPa at room temperature. Steady creep rates measured at a constant load in the range of relatively small strains were described by a stress exponent,  $n$ , of 2 and by an activation energy of  $586 \pm 40 \text{ kJ/mol}$ . Large deformations during the accelerating creep were accompanied by extensive formation of cavities.*

Yttria-tetragonal ZrO<sub>2</sub> polycrystals (Y-TZP) is considered to be one of the most promising structural materials for mechanical applications because of their excellent bending strength and fracture toughness. The increase in toughness of TZP at room temperature has been attributed to a stress-induced tetragonal/monoclinic transformation.<sup>1-3</sup> Metastable tetragonal phase is stable when the grain size is below a critical value.<sup>2,3</sup> Fracture toughness and other mechanical properties can be optimized by obtaining polycrystals which consist of very small *t*-ZrO<sub>2</sub> grains (0.2 to 1  $\mu\text{m}$ ) containing  $\approx 3 \text{ mol\% Y}_2\text{O}_3$  in solid solution.

On the other hand, some mechanical properties such as tensile strength or creep resistance at high temperatures were not so good,<sup>4</sup> because the transformational toughening mechanism could not work and plastic deformation, caused by the very small grain size and symmetrical shape of grains, occurred easily. But, if an exceptionally large deformation, superplasticity, is possible, the deformation property can induce many practical applications such as a superplastic forming.

The phenomenon of superplasticity for metal systems has been reviewed by Edington *et al.*<sup>5</sup> Evans *et al.*<sup>6</sup> presented the possibility of superplasticity in ceramics by suppression of cavity formation. Superplastic deformation of very fine-grained ceramics has been observed for UO<sub>2</sub><sup>7</sup> and MgO<sup>8</sup> in compression tests. Moreover, pure zirconia<sup>9</sup> and some ceramics<sup>10,11</sup> have been reported to show the transformational superplasticity in which the deformation was induced by thermal cycling of materials at their transformation temperatures. But, the superplasticity in structural ceramics such as SiC, Si<sub>3</sub>N<sub>4</sub>, or toughened zirconia ceramics has not yet been found.

In this paper, uniaxial tensile deformation properties of Y-TZP (3 mol% Y<sub>2</sub>O<sub>3</sub>) have been investigated at temperatures ranging from 1000° to 1500°C, where the tetragonal phase of zirconia is considered to be stable during the creep deformation. Extensive elongation resulting from structural superplasticity has been observed at a restricted temperature range and a restricted strain rate for this high-performance ceramic.

## EXPERIMENTAL PROCEDURE

### SPECIMEN PREPARATION

The Y-TZP specimens\* were fabricated by sintering the very fine-grained coprecipitated zirconia powder which contained 3 mol% of yttria in solid solution. The sintered material consisted of  $\approx 90\%$  of tetragonal phase grains (*t*-ZrO<sub>2</sub>) and 10% of cubic phase grains (*c*-ZrO<sub>2</sub>)  $\approx 0.3 \mu\text{m}$  in size. Some material properties are shown in Table I. Uniaxial tensile creep specimens were diamond-machined from sintered plates (15 by 100 by 4 mm). The specimen had a gage length of 30 mm with a circular cross section  $\approx 3 \text{ mm}$  in diameter. "Targets" on both sides of the gage-length portion of the specimen were designed so that the creep strain could be measured by a noncontacting electrooptical extensometer.

### TESTING PROCEDURE

Tensile tests at a constant displacement rate were conducted using a universal testing machine<sup>†</sup> in air at 1450°C at a

\*Member, the American Ceramic Society.

\*YTZ, Nippon Kagaku Togyo Co., Ltd., Sakai, Japan.

†Instron Corp., Canton, MA.

Received September 3, 1985; approved March 20, 1986.

Table I. Properties of Y-TZP (rt)

Density	6.04 g/cm <sup>3</sup>
Tetragonal phase	90%
Grain size	0.3 $\mu\text{m}$
Young's modulus	206 GPa
Poisson's ratio	0.31
Bending strength	1200 MPa
Fracture toughness	6-7 MN/m <sup>3/2</sup>

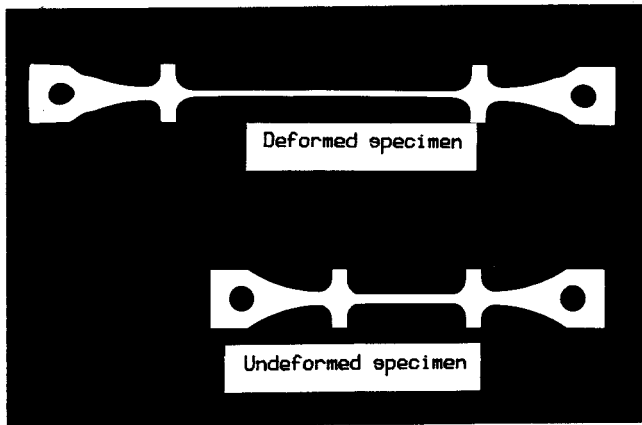


Fig. 1. Superplastically elongated specimen of Y-TZP at 1450°C.

cross-head speed of 0.05 to 1.0 mm/min. The elongation of the specimen was estimated by the displacement of the cross-head.

Tensile creep tests at a constant load were performed in air at temperatures up to 1500°C. The testing apparatus has been described elsewhere.<sup>12</sup> The specimen was gripped by newly designed chucking devices which were made of sintered SiC. The creep deformation of the specimen was measured using an electrooptical extensometer having the resolution of 5 μm. The surface of deformed tensile specimens was examined by scanning electron microscopy.

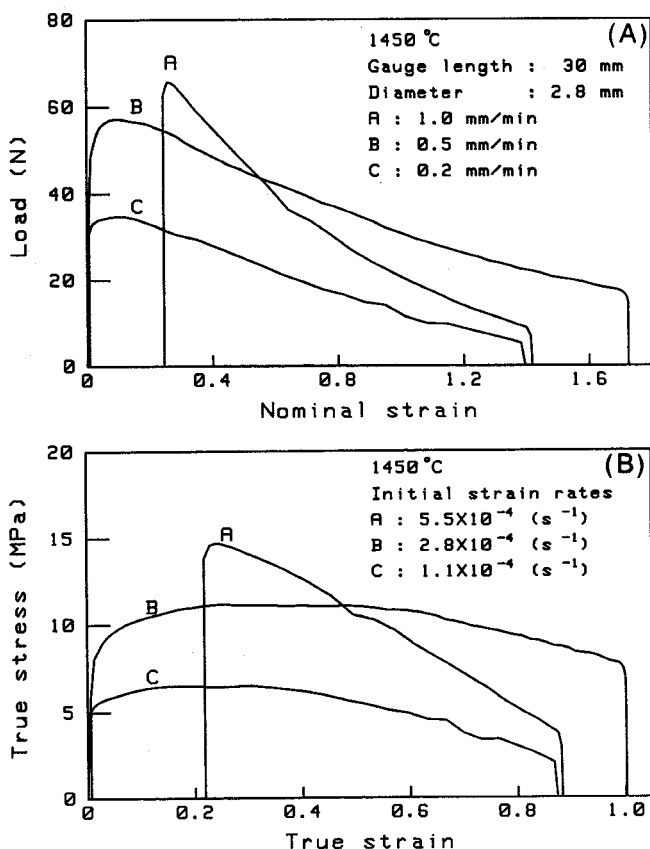


Fig. 2. (A) Typical load-nominal strain curves under constant displacement rate. (B) Estimated true stress-true strain curves by assuming a uniform deformation without local necking.

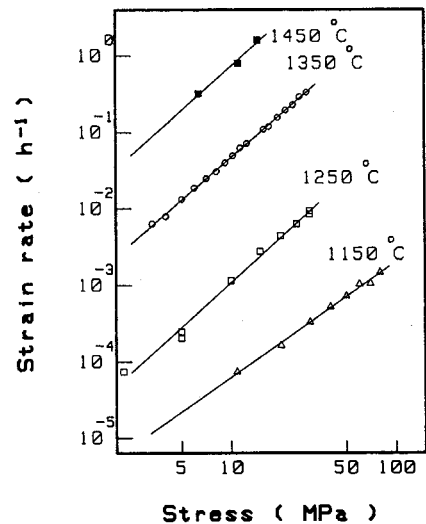


Fig. 3. Steady-state creep rate vs applied stress for Y-TZP.

## RESULTS

### TENSILE TEST AT A CONSTANT DISPLACEMENT RATE

The superplastically deformed specimen of Y-TZP which showed >120% elongation is presented in Fig. 1; the undeformed specimen is also shown for comparison. Elongation at the gage-length portion was uniform and local necking was not observed. Load-strain curves at 1450°C with various cross-head speeds are shown in Fig. 2(A). The specimen which was strained at the cross-head speed of 1 mm/min had been deformed by 23% prior to the tensile test. Loads decreased during these tests because of the reduction of specimen cross-section and the reduction of effective strain rate with the extent of deformation.

True strain,  $\epsilon_t$ , is defined as

$$\epsilon_t = \ln(l/l_0), \quad (1)$$

where  $l$  and  $l_0$  are the elongated gage length and the original gage length, respectively. By assuming there is no local necking, true stress,  $\sigma_t$ , can be calculated by the following relation:

$$\sigma_t = S \exp(\epsilon_t) \quad (2)$$

where  $S$  is the nominal stress ( $S = P/A_0$ ),  $P$  the applied load, and  $A_0$  the cross section of the original specimen. True stress vs true strain curves are shown in Fig. 2(B). True stresses reached maximum values at the true strain of  $\approx 0.3$  then gradually decreased with elongation. True stress of the specimen deformed at the cross-head speed of 1 mm/min decreased rapidly with deformation.

The bending strength of superplastically deformed specimens was examined at room temperature. Bend specimens were cut from the gage-length portion of tensile specimens with the elongation of 120% whose diameters were 1.8 mm. The three-point bending strength (span 18 mm) of the deformed specimen which had been strained at 1 mm/min was 470 MPa, and that of the deformed specimen which had been strained at 0.2 mm/min was 976 MPa.

### TENSILE CREEP AT A CONSTANT LOAD

*Creep Properties at Small Strain.* The relation between stress and strain rate was obtained by the rapid change of testing stresses. All experiments were conducted with the deformation of <20%. Stress and strain rate curves are plotted in Fig. 3. Strain rate is described by an equation of the following form

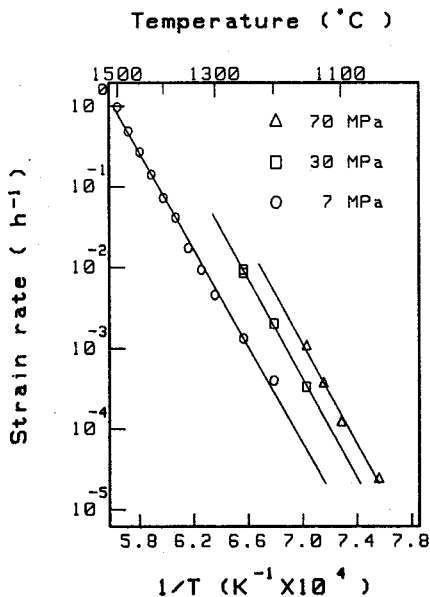


Fig. 4. Steady-state creep rate vs reciprocal absolute temperature for Y-TZP.

$$\dot{\epsilon} = A\sigma^n \exp(-\Delta Q/RT) \quad (3)$$

where  $n$  is the stress exponent and  $\Delta Q$  the activation energy. The stress exponents for 1150°, 1250°, and 1350°C were 1.5, 1.9, and 1.9, respectively. The data points for 1450°C in Fig. 3 were obtained from the maximum true stresses during the tensile tests at a constant displacement rate. These data also gave a stress exponent of 1.9, nearly equal to 2.

The temperature dependence of creep strain rate was obtained by the rapid change of testing temperatures. Logarithmic plots of strain rate vs  $1/T$  gave a linear relation in the range of temperatures for 70, 30, and 7 MPa were calculated to be 590, 590, and 573 kJ/mol, respectively.

**Creep Properties at Large Strain.** Constant load creep curves were recorded until the final fracture occurred. Typical creep curves at 1350° and 1450°C with a constant load corresponding to the nominal stress of 7 MPa are shown in Fig. 5. Final creep deformation of the specimen which was tested at 1350°C exceeded nominal strain of 100% at fracture. The remarkable characteristic of the creep curves was that the extent

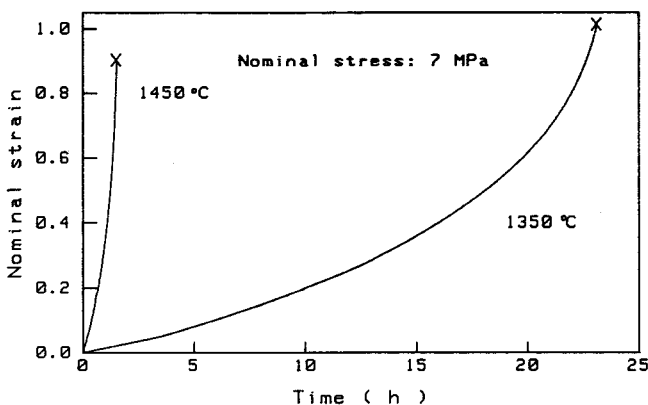


Fig. 5. Typical creep curves with a constant load corresponding to the nominal stress of 7 MPa showing large deformations during the accelerating creep.

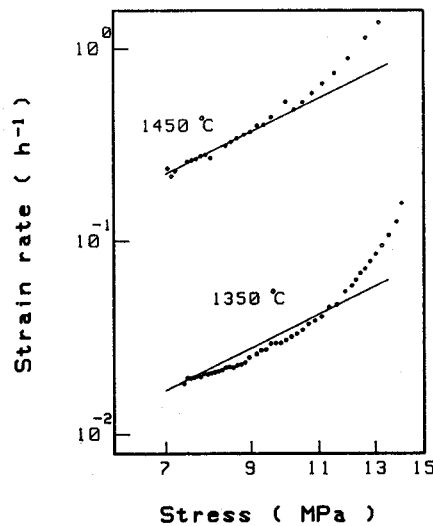


Fig. 6. True strain rate vs true stress calculated from the deformation curves.

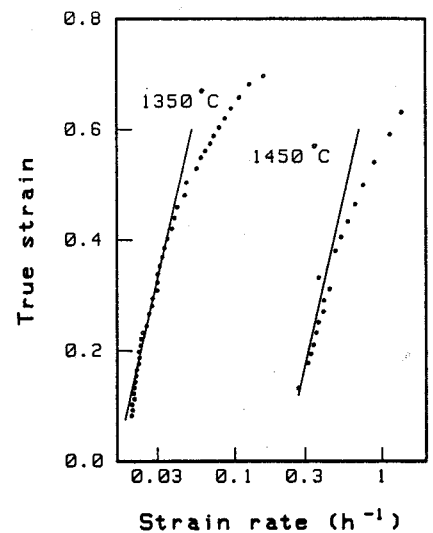


Fig. 7. True strain vs true strain rate calculated from the deformation curves.

of deformation during the accelerating creep period was very large. Acceleration of the creep rate was partly caused by the reduction of specimen cross section with the elongation and the increase of true stress. True strain rate vs true stress calculated from the deformation curves is plotted in Fig. 6. Straight lines indicate the stress exponent of 2, which was obtained by creep tests at low strain. Apparent stress exponents exceeded 4 when effective stresses became high. The relation between true strain and true strain rate is shown in Fig. 7. Plotted curves tended to deviate gradually from the linear relation when true strain increased, exceeding 0.3.

#### MICROSTRUCTURAL ANALYSIS

The extensive cavitation was observed on the surface of the tensile specimen which was deformed up to nominal strain of 120% with the displacement rate of 1 mm/min at 1450°C (Fig. 8). The creep-ruptured surface of this specimen showed entirely intergranular fracture (Fig. 9). The surface of the specimen elongated at a slower rate, 0.2 mm/min, showed less

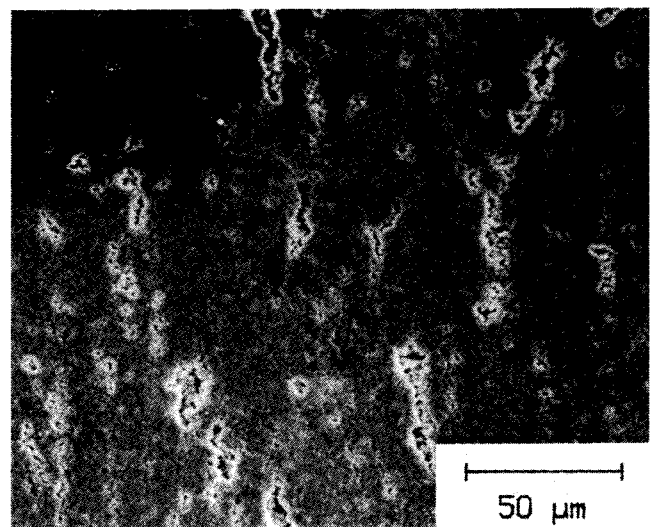


Fig. 8. SEM micrograph of cavitation on the surface of tensile specimen elongated >120% with 1 mm/min at 1450°C.

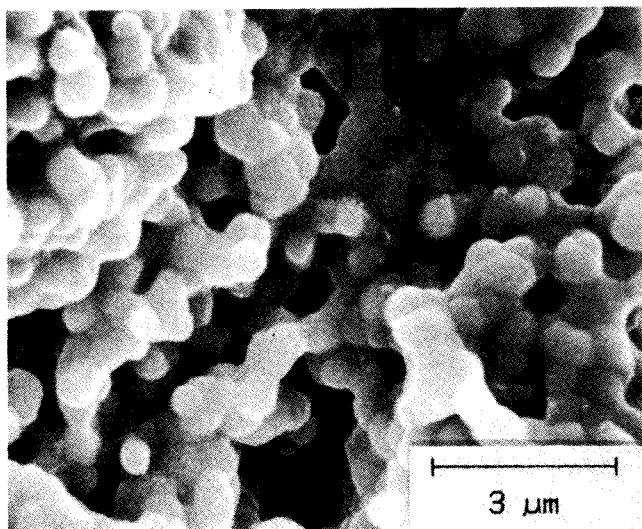


Fig. 9. SEM micrograph of fracture surface of the ruptured specimen showing intergranular fracture and cavitation.

cavitation. The grain growth was observed during the superplastic deformation at 1450°C, but each grain maintained the equiaxed shape.

The microstructure of the deformed specimen which was strained up to 24% at 1250°C showed no change in grain size or grain shape, compared with the original specimen. Thus it was ascertained that the creep deformation was caused neither by the grain growth nor by elongation of individual grains. These results indicated that the deformation can be explained by the grain-boundary sliding mechanism.

## DISCUSSION

### DEFORMATION AT SMALL STRAIN

Creep properties of various zirconia polycrystals are summarized in Table II.<sup>13-16</sup> Several workers investigated creep properties of Y<sub>2</sub>O<sub>3</sub>-fully stabilized zirconia (Y-FSZ) with large average grain size. Fehrenbacher *et al.*<sup>16</sup> observed creep rates as small as  $3.9 \times 10^{-5} \text{ h}^{-1}$  at 1475°C under 4.4 MPa in air for Y-FSZ with grain size of 18 μm. The present results obtained under the same conditions for Y-TZP was  $1.9 \times 10^{-1} \text{ h}^{-1}$ . The enhanced creep rate can be attributed to the small grain size of the Y-TZP (0.3 μm). Therefore, the difference in creep rates between two materials could be explained by the assumption that the creep strain rate is proportional to the inverse square of the grain size.

Previous studies indicated that the creep was attributed to the grain-boundary sliding controlled by diffusion of cations.<sup>13-16</sup> The measured stress exponent of 2 and microstructural analysis suggest the validity of the grain-boundary sliding mechanism for this material. The flow stress of structurally superplastic materials is described by the following equation as a function of strain rate

$$\sigma = K\dot{\epsilon}^m \quad (4)$$

where  $K$  is a constant and  $m$  is the strain rate sensitivity index. The superplastic regime is the region where  $m$  is  $>0.3$ . The  $m$  value of 0.5 which corresponds to the stress exponent of 2 is considered to be one indication of superplasticity.

Grain-boundary sliding is considered to be accommodated by diffusion or by dislocation. Although diffusion properties of  $t\text{-ZrO}_2$  are unknown, certain analyses of creep properties of Y-TZP can be done using diffusion data obtained for stabilized  $c\text{-ZrO}_2$  which is isostructural to CaF<sub>2</sub> or UO<sub>2</sub>. Oishi *et al.*<sup>17</sup> represented Y-Zr interdiffusion coefficients of Y<sub>2</sub>O<sub>3</sub>-stabilized zirconia as follows

$$\bar{D}_{\text{Y-Zr}} = 2.7 \times 10^{-1} \exp(-423(\text{kJ/mol})/RT) \text{ cm}^2/\text{s} \quad (5)$$

$$\delta\bar{D}'_{\text{Y-Zr}} = 1.2 \times 10^{-6} \exp(-293(\text{kJ/mol})/RT) \text{ cm}^3/\text{s} \quad (6)$$

where  $\bar{D}$  and  $\delta\bar{D}'$  are the lattice and grain-boundary interdiffusion coefficients, respectively. The activation energy of the lattice self-diffusion coefficient was 439 kJ/mol for Zr<sup>4+</sup> and 391 kJ/mol for Y<sup>3+</sup>. Apparent creep activation energies do not coincide with these activation energies for diffusion. Seltzer and Talty<sup>14</sup> suggested that the creep activation energy is equal to the sum of the self-diffusion energies for cation and anion species. An activation energy of 127 kJ/mol for oxygen diffusion<sup>18</sup> gives apparent activation energy of 566 kJ/mol if the former value is added to the activation energy for Zr<sup>4+</sup> diffusion coefficient.

As for dislocation motion, Mecartney *et al.*<sup>19</sup> indicated that the {001}  $\langle\bar{1}10\rangle$  was the primary slip system for single-crystal CaO-stabilized zirconia and extensive dislocation climb took place from 1350° to 1450°C. When the fact that the creep deformation of fine-grained Y-TZP occurs far below the yield stress is considered, dislocation glide alone does not seem to be the major mechanism of the deformation. It is believed that the enhanced grain-boundary diffusion of cations combined with dislocation climb are the accommodation mechanisms of grain-boundary sliding.

### EFFECT OF CAVITATION AT LARGE STRAIN

By granting the power law relation between stress and strain rate (Eqs. (2) and (4)), the constant-load creep curve can be described by the following equation

$$\epsilon = \ln(K/S) + m \ln(\dot{\epsilon}) \quad (7)$$

Straight lines in Fig. 6 indicate the deformation behaviors predicted by Eq. (7). This relation, however, does not satisfy the experimentally obtained curves in the strain range  $>0.3$ . The microstructural change caused by extensive cavitation at large strain may lead to the accelerating creep rate which deviates from the relation described in Eq. (7).

Although effects of cavitation for creep curves have been observed at strains  $>0.3$ , specimens could be elongated over 100% without fracture. If the surface diffusivities of the system are sufficiently high, the cavities can retain equilibrium shape and avoid development of a crack-like cavity.<sup>6,7</sup> The present authors believe that large, superplastic deformation can be achieved under conditions of stable cavity formation or the stable pore growth.

Table II. Creep Properties of Various Zirconia Ceramics

Material	Y <sub>2</sub> O <sub>3</sub> (mol%)	Grain size (μm)	$n$	Activation energy (kJ/mol)	Ref.
Y-FSZ	5.8	15-20	1.5		16
Y-FSZ	6	17	1.6	360 ± 120	13
Y-FSZ	5.8-9.7	29-40	1.5	534 ± 40	14
Y-TZP	3	0.3	2	586 ± 40	Present work

## CONCLUSIONS

The present report has shown that Y-TZP (grain size  $0.3 \mu\text{m}$ ) could be elongated superplastically  $>120\%$  with the right combination of temperature and strain rate. Even though extensive cavitation has been observed in the deformed specimens strained rapidly, the superplastically deformed material strained at a slower rate maintained a bending strength of 976 MPa at room temperature. Creep deformation properties at low strain have been described by Eq. (3). The stress exponent was 2 in the temperature range  $1150^\circ$  to  $1450^\circ\text{C}$ , and the activation energy obtained at the stress level from 7 to 70 MPa was  $586 \pm 40 \text{ kJ/mol}$ . Strain rate was considered to be proportional to the inverse square of the grain size.

Deformation properties at large strain were affected by the cavitation. The apparent stress exponent exceeded 4 under large strain. The observed accelerating creep region in constant-load creep curve was attributed to the reduction of specimen cross section and to the effect of cavitation. The amount of cavitation during deformation was reduced by controlling the strain rate and the temperature.

## ACKNOWLEDGMENTS

The Y-TZP samples were kindly provided by T. Kawanami of Nippon Kagaku Togyo Co. Ltd. The authors would like to thank S. Sakai for specimen preparation and T. Oji for designing chucking devices. Thanks are also due to S. Kanzaki and K. Hayakawa for their helpful discussions.

## REFERENCES

- <sup>1</sup>T. K. Gupta, J. H. Bechtold, R. C. Kuznicki, and L. H. Cadoff, "Stabilization of Tetragonal Phase in Polycrystalline Zirconia," *J. Mater. Sci.*, **12**, 2421–26 (1977).
- <sup>2</sup>T. K. Gupta, F. F. Lange, and J. H. Bechtold, "Effect of Stress-Induced Phase Transformation on the Properties of Polycrystalline Zirconia Containing Metastable Tetragonal Phase," *ibid.*, **13**, 1464–70 (1978).
- <sup>3</sup>F. F. Lange, "Transformation Toughening-Part 3, Experimental Observations in the  $\text{ZrO}_2\text{-Y}_2\text{O}_3$  System," *ibid.*, **17**, 240–46 (1982).
- <sup>4</sup>K. Matsusue, Y. Fujisawa, and K. Takahara, "Tensile Strength of Hot-Pressed  $\text{ZrO}_2\text{-Y}_2\text{O}_3$  at High Temperature," *Yogyo-Kyokai-Shi*, **91** [1] 59–61 (1983).
- <sup>5</sup>J. W. Edington, K. N. Melton, and C. P. Cutler, "Superplasticity"; pp. 61–170 in *Progress in Materials Science*, **21**, 1976.
- <sup>6</sup>A. G. Evans, J. R. Rice, and J. P. Hirth, "Suppression of Cavity Formation in Ceramics: Prospects for Superplasticity," *J. Am. Ceram. Soc.*, **63** [7-8] 368–75 (1980).
- <sup>7</sup>T. E. Chung and T. J. Davies, "Pore Behavior in Fine-Grained  $\text{UO}_2$  During Superplastic Creep," *Creep. Fract. Eng. Mater. Struct.*, **395–407** (1981).
- <sup>8</sup>J. Crampon and B. Escaig, "Mechanical Properties of Fine-Grained Magnesium Oxide at Large Compressive Strains," *J. Am. Ceram. Soc.*, **63** [11-12] 680–86 (1980).
- <sup>9</sup>J. L. Hart and A. C. D. Chaklader, "Superplasticity in Pure  $\text{ZrO}_2$ ," *Mater. Res. Bull.*, **2**, 521–26 (1967).
- <sup>10</sup>C. A. Johnson, R. C. Bradt, and J. H. Hoke, "Transformational Superplasticity in  $\text{Bi}_2\text{O}_3$ ," *J. Am. Ceram. Soc.*, **58** [1-2] 37–40 (1975).
- <sup>11</sup>L. A. Winger, R. C. Bradt, and J. H. Hoke, "Transformational Superplasticity of  $\text{Bi}_2\text{WO}_6$  and  $\text{Bi}_2\text{MoO}_6$ ," *ibid.*, **63** [5-6] 291–94 (1980).
- <sup>12</sup>F. Wakai, S. Sakaguchi, Y. Matsuno, and H. Okuda, "Tensile Creep Test of Hot-Pressed  $\text{Si}_3\text{N}_4$ "; pp. 279–85 in *Proc. First Int'l. Symp. on Ceramic Components for Engines*. Edited by S. Somiya, E. Kanai, and K. Ando. KTK Scientific, Tokyo, and D. Reidel, Boston, 1984.
- <sup>13</sup>P. E. Evans, "Creep in Yttria- and Scandia-Stabilized Zirconia," *J. Am. Ceram. Soc.*, **53** [7] 365–69 (1970).
- <sup>14</sup>M. S. Seltzer and P. K. Talty, "High-Temperature Creep of  $\text{Y}_2\text{O}_3$ -Stabilized  $\text{ZrO}_2$ ," *ibid.*, **58** [3-4] 124–30 (1975).
- <sup>15</sup>M. S. Seltzer and P. K. Talty, "Creep of Low-Density Yttria/Rare Earth-Stabilized Zirconia"; in *Deformation of Ceramic Materials*. Edited by R. C. Bradt and R. E. Tressler, Plenum, 1975.
- <sup>16</sup>L. L. Fehrenbacher, F. P. Bailey, and N. A. McKinnon, "Compressive Creep of Yttria Rare Earth Stabilized Zirconia Storage Heat Refractories," *SAMPE Quart.*, **2** [4] 48–60 (1971).
- <sup>17</sup>Y. Oishi, K. Ando, and Y. Sakka, "Lattice and Grain-Boundary Diffusion Coefficients of Cations in Stabilized Zirconias," *Advances in Ceramics*, Vol. 7. American Ceramic Society, Columbus, OH, 1983.
- <sup>18</sup>L. A. Simpson and R. E. Carter, "Oxygen Exchange and Diffusion in Calcia-Stabilized Zirconia," *J. Am. Ceram. Soc.*, **49** [3] 139–44 (1966).
- <sup>19</sup>M. L. McCartney, W. T. Donlon, and A. H. Heuer, "Plastic Deformation in CaO-Stabilized  $\text{ZrO}_2(\text{CSZ})$ ," *J. Mater. Sci.*, **15** [4] 1063–65 (1980). □